Catalysis Science & Technology

Accepted Manuscript

ROYAL SOCIETY OF CHEMISTRY

www.rsc.org/catalysis

Cite this: DOI: 10.1039/c0xx00000x

www.rsc.org/xxxxxx

ARTICLE TYPE

The effects of Pd chemical state on the activity of Pd/Al_2O_3 catalysts in CO oxidation

Yanhui Zhang, Yafeng Cai, Yun Guo*, Haifeng Wang, Li Wang*, Yang Lou, Yanglong Guo, Guanzhong Lu, Yanqing Wang

Received (in XXX, XXX) XthXXXXXXXXX 20XX, Accepted Xth XXXXXXXXX 20XX
DOI: 10.1039/b000000x

CO adsorption and O_2 activation played important role in CO oxidation on supported Pd catalyst, which was depended on the chemical state of Pd. A series supported Pd on Al_2O_3 catalysts with different state were prepared: metal Pd (NCR), PdO (NC), Pd^{2+} coordinated with Cl^- (Pd^{2+}-Cl^-, CF), and the mixture of PdO and Pd^{2+}-Cl^- (CC), the activity of CO oxidation was in the order of NCR ~ CF > CC >>NC. The catalysts were characterized by BET, XRD, H_2-TPR, XPS and In-situ DRIFTS. The results showed that the metal Pd (Pd^0) could be partially oxidized to Pd^+ in the presence of O_2, which producing the new CO adsorption sites and decreasing CO adsorption strength simultaneously. The cooperation of enhancement of CO adsorption amount and decrease of CO adsorption strength led to high activity for CO oxidation on NCR. For Pd existed in the species with high chemical valence (Pd^{2+}), the chemical environment or coordinated ligand of Pd species showed great effects on the CO oxidation. The lowest CO oxidation activity on NC was induced by that PdO hardly adsorbed CO, meanwhile, PdO was difficult to be reduced by CO. However, the existence of Cl^- significantly promoted the reduction of Pd^{2+} to Pd^+, which increasing the CO adsorption amount and resulting in the higher activity for CO oxidation on CF and CC than PdO. Tuning the CO adsorption by adjusting chemical state of Pd may be a useful approach to prepare the highly efficient supported Pd catalyst.

1. Introduction

CO oxidation has drawn great attention due to its wide applications, such as automotive emission control and CO preferential oxidation for proton exchange membrane fuel cells (PEMFC)[1-5]. Supported noble metal catalysts have been proved to be effective for CO oxidation and have been widely studied [6-15]. Since the pioneering work by Haruta[10], nano-gold catalyst was regarded as the catalyst with the highest activity for low temperature CO oxidation. However, the direct applications of supported Au catalysts in the commercial processes have been hampered by several unsolved problems[16, 17]. Supported Pt and Pd catalysts are the most active catalysts at the high temperature[6, 18, 19], for example used in car exhaust after-treatment, but showed poor activities for low temperature CO oxidation, which origined from the competition between CO adsorption and the formation of active oxygen. For example, too strong CO adsorption on Pt surface blocked the active sites for oxygen adsorption and activation, namely CO poison effect, especially at low temperature[8, 20]. In order to improve the activities of Pd and Pt, a method for providing the extra activesites of oxygen activation on the catalyst was adopted to improve the catalytic activity of noble metals for CO oxidation. For instance, growing FeO_x on Pt (111) could supply the extra active sites for O_2 activation for Pt catalyst with the help of FeO_x[21], supported Pd on $Fe(OH)_x$ showed comparable activity of CO oxidation with nano-gold catalyst[22-25].

Nørskov et al. [18] calculated the Sabatier activity of CO oxidation on Pd, Pt, Cu, Ag and Au, giving the upper bound of reaction rate. The results showed that the adsorption energy of CO and atomic O (scaling linearly with the adsorption energy of O_2) decided the Sabatier rate of CO oxidation, providing an idea to improving CO oxidation activity of Pd by decreasing the adsorption energy of CO and O_2 .

The adsorption of CO and the activation of O_2 are significantly influenced by the chemical state of Pd[26-30]. For example, metal Pd could adsorb CO on the hole, bridge and top sites, and O_2 on the adjacent adsorption sites[31, 32]. CO hardly adsorbed on the surface of PdO[31], and the O_2 adsorption also obviously declined due to the Pd surface having positive charge[33, 34]. Meanwhile, the reaction atmosphere, temperature and etc. could induce the transformation between different Pd states, showing great effects on CO oxidation. Rupprechter[31] et al. reported the rapid reduction of $PdO_{x<1}$ to Pd upon CO exposure. Goodman[35, 36] further found the Pd oxide surface with lower exposure of O_2 formed more defects, which adsorbed more CO and showed stronger interaction with CO, exhibited enhanced reactivity for CO oxidation. Compared with PdO[37], our recent results of CO oxidation on $PdCl_2$-$CuCl_2/Al_2O_3$ showed $PdCl_2$ was easily reduced to Pd^+ by CO[38-40], which indicated the chemical environment or the coordinated ligand of Pd could greatly

influence the redox properties of Pd and the existence form of Pd species in the reaction, playing important role in CO oxidation.

In this work, we prepared the supported Pd catalysts with different state and investigated the effects of Pd chemical state on the low temperature CO oxidation. XRD, XPS, H_2-TPR and In-situ DRIFTS were used to gain insight into the roles of Pd chemical state in CO oxidation.

2. Experimental

2.1 Materials

Absolute ethyl alcohol (CP) was from Sinoharm Chemical Reagent Co., Ltd.; $Pd(NO_3)_2$(AR) was from Heraeus Materials Technology Shanghai Ltd.; Al_2O_3(BET surface area of 194 m^2/g) was from Yang-Zhou Baisheng Catalyst Co., Ltd.

2.2 Catalyst preparation

Supported Pd catalyst was prepared by wetness impregnation method with aqueous $Pd(NO_3)_2$ solution as Pd precursor. Briefly, 0.216 g $Pd(NO_3)_2$ was dissolved in 8ml de-ionized water and 2 ml absolute ethyl alcohol. 5 g Al_2O_3 was impregnated in this solution. After aging under stirring for 2 h, the catalyst was dried at 40 ^oC by reduced pressure distillation through rotary evaporator, then calcined in 50 vol.% O_2/N_2 gas flow (50 ml/min) at 550 ^oC for 3 hours. The obtained catalyst was denoted as NC. NC was further reduced by pure hydrogen (40 ml/min) at 200 ^oC for 3 hours to obtain NCR catalyst. Another supported Pd catalyst using HCl solution of $PdCl_2$ as precursor was prepared in the same way. The catalysts before and after calcination were denoted as CF and CC, respectively.

2.3 Catalyst characterization

The specific surface areas of the catalysts were determined by nitrogen adsorption at 77.4 K using a NOVA 4200e instrument. Prior to each measurement, the samples were vacuumed at 180 ^oC for 10 h.

Actual Pd loading were measured by an ICP-AES instrument (Varian 710). The amounts of chlorine or nitrogen in the catalysts were determined by X-ray fluorescence instrument (XRF-1800) and elemental analyser (German elementarvario EL III), respectively.

The powder X-ray diffraction patterns (XRD) of the catalysts were recorded on a Bruke D8 focus diffraction spectrometer using a Cu Kα radiation (1.54056 Å, 40 Kv and 40mA) over a 2θ range from 20^o to 80^o with a scan rate of 6^o/min.

The X-ray photoelectron spectroscopy (XPS) was performed on a Thermo ESCALAB 250 spectrometer with Al Kα radiation (1486.6 eV). All of the XPS data were calibrated using the binding energy of C 1s (284.6 eV) as standard.

Temperature programmed reduction by hydrogen (H_2-TPR) was performed on a commercial temperature-programming system with 100mg catalyst. The samples were heated in 5 vol.% H_2/N_2 gas flow (45 mL/min) from room temperature to 800 ^oC with a heating rate of 10 ^oC/min.

In-situ diffuse reflectance infrared Fourier transition spectroscopy (DRIFTS) was carried out on a Nicolet Nexus 670 spectrometer equipped with a MCT detector cooled by liquid nitrogen at a spectral resolution of 4 cm^{-1} (accumulating 64 scans). About 40 mg of fine powder catalyst were placed firmly in the diffuse reflectance cell fitted with ZnSe window and a heating cartridge. The catalyst was pretreated in He flow (30ml/min) at 200 ^oC for 1h and cooled down to 30 ^oC for 15 min, then the background spectra were recorded. After pretreatment, the catalyst was exposed to the corresponding gas mixture, the DRIFTS spectra were collected. For CO adsorption, the spectra were recorded after the sample being exposed to 500 ppm CO in Helium (ca.40 mL/min). The mixture of 500 ppm CO and different concentration O_2 in a Helium flow (10, 20 and 40 vol%) was used in the CO oxidation.

2.4 Testing of catalytic activity

The activity of catalyst for CO oxidation was tested in a quartz U-tube (Φ3.5mm) fixed-bed reactor at atmospheric pressure. The temperature was controlled by using vacuum flask with ethanol/liquid nitrogen mixture from -80 ^oC to 10 ^oC, and by warm water bath from 10 ^oC to 100 ^oC. 200 mg catalyst of 20–40 mesh was used for each run. The feed gas consisted of 200 ppm CO and 20 % O_2 balanced with nitrogen passed through the catalyst bed at a flow rate of 30 ml/min, the space velocity was 9000 ml g^{-1} h^{-1}. For kinetic measurements, space velocity was controlled at a range of 9000-60000 ml g^{-1} h^{-1} to limit CO conversion between 5% and 15%. All the activity tests were carried out after the reaction was under steady state condition, CO conversion was measured by an online gas chromatograph.

3. Results

3.1 CO oxidation activity and kinetic measurement on different catalyst

Fig.1 shows the CO oxidation activity of different catalysts. CO could be completely oxidized at 92 ^oC on NC. H_2 pre-reduction greatly promoted the activity of NC, and the complete conversion temperature (T_{100}) of CO was 8 ^oC on NCR, which implied metal Pd behaved higher activity. However, CF, prepared by the deposition of $PdCl_2$ on Al_2O_3, showed surprising high activity, T_{100} was 10^{o}C, which was close to that of NCR. After calcination at 550^{o}C, the activity of CC decreased slightly, T_{100} of CC was 25 ^oC, much lower than that of NC. Table.1 shows the kinetic parameters for CO oxidation over Pd catalysts. TOFs normalized by unit surface Pd atom were compared to gain insight into the intrinsic activities of Pd catalysts. TOF of pre-reduced NCR catalyst was 93.09×10^{-5} s^{-1} at 0 ^oC, much higher than NC catalyst (10.99×10^{-5} s^{-1}). Interestingly, TOFs of CF and CC with high chemical valence of Pd (56.43×10^{-5} and 44.70×10^{-5} s^{-1}) were also much higher than NC. Combined with the results, it could be concluded that the chemical state of Pd, including valence state and coordination environment, showed significant effects on the activity.

Cite this: DOI: 10.1039/c0xx00000x

www.rsc.org/xxxxxx

ARTICLE TYPE

Table 1. The compositions, surface areas, kinetic paratmeters for CO oxidation and surface compositional of Pd in different catalysts

Catalyst	Pd loading (wt%)	N(Cl) amount[a] (wt%)	Surface area (m^2/g)	Dispersion[b] (%)	Pd species size (nm)	r[c] ×10^7 (mol_{CO}•g_{Pd}^{-1}•s^{-1})	TOF×10^5 (s^{-1})	Surface Pd concentration (at.%)	The ratio of different Pd states			
									Pd^0	PdO	Pd^{2+}	Pd^+
NCR	1.80	<0.3	178.7	6.7	20	5.25	93.09	0.91	>99	/	/	/
NC	1.73	<0.3	164.2	6.2	21	0.66	10.99	0.94	/	>99	/	/
CC	1.66	1.70	155.4	15.9	8	6.30	44.70	0.43	/	74	6.5	19
CF	1.72	3.15	165.7	17.0	7	9.02	56.43	0.39	/	/	55	45

[a]N amount was detected by a German elementar vario EL III elementalanalyser, the detection limitation was 0.3%.

[b]Dispersion of Pd was obtained from CO chemisorption at 30 °C, all catalysts were pre-reduced by H_2 at 300 °C for 0.5h before CO chemisaorption.

[c]Reaction rate (r) was obtained at 0 °C.

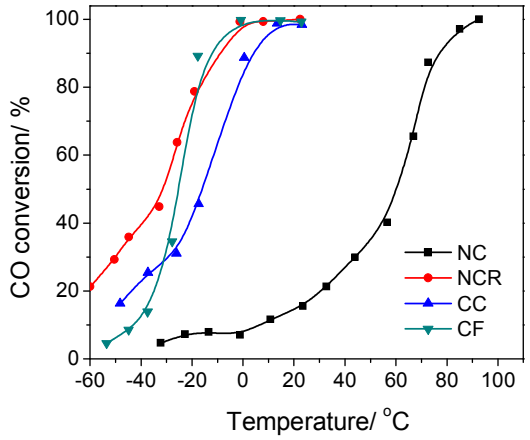

Fig. 1 The catalytic activity of different supported Pd catalysts (200 ppm CO + 20% O_2 balanced with N_2, WHSV 9,000 ml g^{-1}•h^{-1})

3.2 X-ray diffraction and BET surface area

XRD patterns of different catalysts are shown in Fig. 2. The characteristic diffraction peaksof PdO were detected at 33.8, 42.2, 54.9 and 71.7° on NC catalyst [41-43], which indicated the growth of PdO particles in the process of calcination. After H_2 reduction, the NCR pattern showed a diffraction peak at 40.12 °, which was attributed to metallic Pd species[42]. The particle sizes of PdO/Pd in NC and NCR calculated based on Debye-Scherrer formula were about 20 nm, which were close to that derived from CO chemisorption (Table 1). However, no characteristic peaks of $PdCl_2$ or PdO were detected on CF and CC catalysts, which indicated $PdCl_2$/PdO was highly dispersed on the support surface. It was because that Al_2O_3 surface was positive charged due to the lower pH value of impregnation solution ($Pd(NO_3)_2$ solution or HCl solution of $PdCl_2$) than PZC of Al_2O_3, which was available for the dispersion of Pd species with negative charge on the support surface through electrostatic attraction[44]. The dominant Pd species was $PdCl_4^{2-}$ anion in HCl solution of $PdCl_2$ and Pd^{2+}cation in $Pd(NO_3)_2$ solution. Therefore, the dispersion of Pd species on Al_2O_3 support were effectively promoted when HCl solution of $PdCl_2$ was used as precursor.

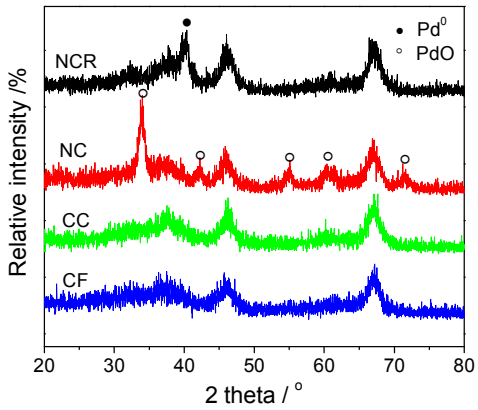

Fig. 2. XRD patterns of supported Pd catalysts

3.3 X-ray photoelectron spectroscopy

Pd 3d XPS spectra and surface composition of the catalysts are shown in Fig.3 and Table.1. The Pd loadings determinated by ICP-AES were close to 1.7% in all catalysts (Table 1). However, the surface concentration of Pd on CC or CF was about half of that on either NC or NCR (Table 1). The XRD results have confirmed the Pd species were highly dispersed on the surface of CC and CF. Therefore, the lower surface concentration of Pd on CC and CF was believed to be aroused by the transfer of Pd species into the inner pore of supports.

Pd $3d_{5/2}$ binding energy (B. E.) of NC is 336.7 eV, corresponding

to PdO species[45-47]. After being reduced to metallic Pd (Pd^0) by H_2, the B. E. of Pd $3d_{5/2}$ in NCR shifted to 335.0 eV[42, 46]. However, two states of Pd were observed on CF at B.E. of 337.6 and 335.8 eV, which could be ascribed to Pd^{2+} and Pd^+, respectively[39]. Meanwhile, the B. E. of Pd^{2+} in CF was higher than that of PdO in NC which was induced by the existence of Cl^- on the CF surface (Table 1). Cl^- modified the chemical state of Pd and decreased the electron density around Pd due to the stronger electronegativity of Cl^-. It was implied that the chemical environment of Pd could be effectively adjusted through the different coordination environment. After calcinations in the air, the states of Pd in CC became more complex, PdO was detected at the B. E. of 336.8eV except Pd^{2+} and Pd^+, but the surface contents of Pd^{2+} and Pd^+ decreased significantly, which indicated that most of Pd^{2+} and Pd^+ (coordinated with Cl^-) transferred to PdO during the calcinations.

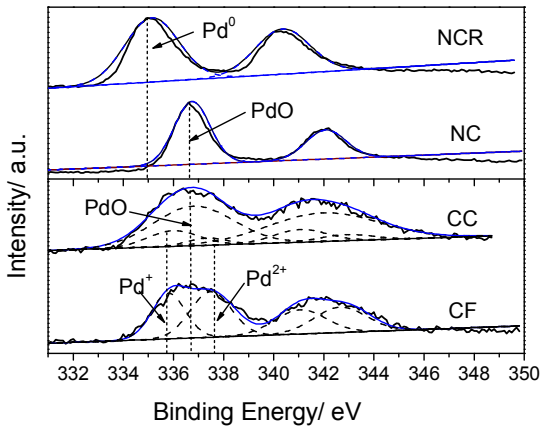

Fig.3 XPS spectra of Pd in different catalysts

3.4 H_2-temperature programmed reduction

H_2-TPR results showed that two hydrogen consumption peaks were observed on NC at 48 and 81 °C, the area of former peak was much bigger than that of latter (Fig. 4). In general, PdO could be reduced to metallic Pd at the temperature lower than 200 °C [48], and the particle size of PdO and the properties of support had significant effect on the reduction temperature of PdO. The bigger PdO particles were easier to be reduced by H_2 than smaller ones due to the less interaction with the support[41-42]. Hence, the low temperature reduction peak of NC was suggested to be the reduction of large PdO particles, and the high temperature reduction was the contribution of the small Pd oxide phase having stronger interactions with support[49, 50].

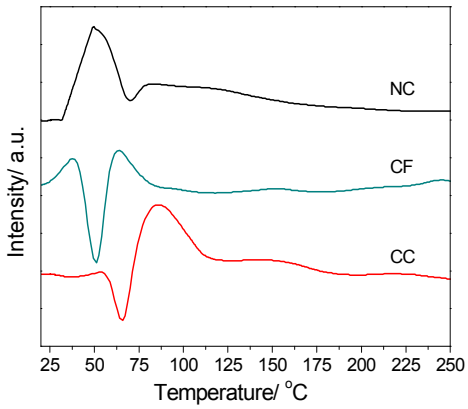

Fig.4 H_2-TPR profiles of NC, CF and CC

Compared with NC, CF catalyst showed different reduction performance, the reduction temperature shifted to lower temperature, and three peaks were detected including two positive peaks at 39 and 65°C and one negative peak at 51 °C. The negative peak was the characteristic of decomposition of the β-PdH phase [50, 51], representing the presence of metallic Pd particles. At the same time, the amount of H_2 consumed on CF, corresponding to the total area of two positive peaks, were much less than that of NC, implying that some Pd species had been reduced before TPR experiment. Combined with the results of XPS, it was suggested that the presence of Cl^- promoted the reduction of Pd species on the CF.

After calcination, a negative peak and a positive peak were detected at 66 and 86 °C on CC, respectively, which corresponded to H_2 desorption [50, 51] and the reduction of Pd species. The desorption peak of H_2 indicated part of Pd species in CC still can be easily reduced below ambient temperature. Combined with the XPS result, the easily reduced Pd species could be conjectured as the Pd^+ or Pd^{2+} species coordinated with Cl^-. Compared with NC, the reduction peak area of CC in the temperature range of 70-150 °C increased significantly, which indicated the more PdO particles with smaller size existed on CC.

Cite this: DOI: 10.1039/c0xx00000x

www.rsc.org/xxxxxx

ARTICLE TYPE

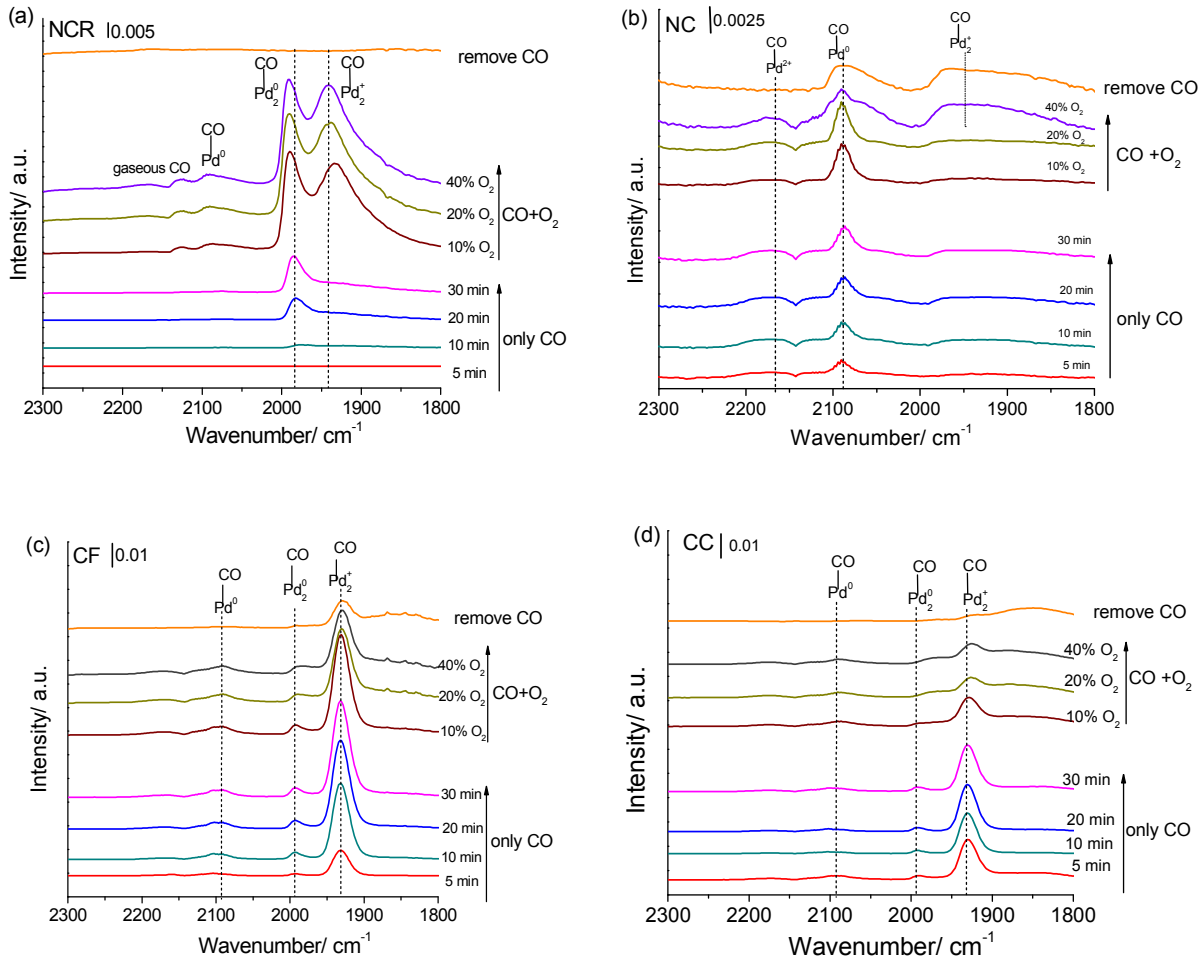

Fig. 5 In situ DRIFTS spectra of the adsorption of CO and CO/O2 on the catalyst of (a) NCR, (b) NC, (c) CF and (d) CC

3.5 In-situ diffuse reflectance infrared Fourier transition spectroscopy (DRIFTS)

In-situ DRIFTS was used to observe CO adsorption on the catalysts, the results are shown in Fig. 5. In these DRIFT spectra, peaks at 2150-2160 cm^{-1} are associated with linear carbonyl groups in Pd^{2+} complexes (Pd^{2+}-CO)[52, 53]; the peaks at 1930–1940 cm^{-1} are related with bridged carbonyl ligands in Pd^{+} complexes (Pd^{+}_2–CO)[54]; bands at 2090 cm^{-1}, 1990 cm^{-1} and broad peaks at 1810 cm^{-1} can be assigned to CO adsorption bands on metallic Pd, which corresponding to the linear carbonyl (Pd^{0}-CO), bridge-bonded carbonyl (Pd^{0}_2-CO) and triply bonded carbonyl complexes(Pd^{0}_3-CO), respectively[52, 54]. Gaseous CO_2 have adsorption peaks at 2350 cm^{-1}[41, 53]and gaseous CO give peaks at 2170 and 2120cm^{-1}[41, 55].

For CO adsorption on NCR catalyst, as can be seen in Fig. 5a, a strong peak corresponded to Pd^{0}_2-CO (the sharp band at 1985 cm^{-1}) were detected,and the intensity of vibration peak increased with the increasing of CO adsorption time, which indicated that bridge sites are more favored for CO chemisorption than top sites on Pd, this result is consistent with a DFT study by Hu[32]. After the introduction of O_2 in the inlet gas, a new strong peak assigned to Pd^{+}_2–CO (1930 cm^{-1}) and a weak peak of Pd^{0}-CO were observed, and the intensity of Pd^{0}_2-CO peak enhanced significantly, which revealed O_2 in the flow not only oxidized part of Pd^{0} to Pd^{+} but also greatly promoted the adsorption of CO on the bridge sites of Pd. At the same time, the blue shift of Pd^{0}_2-CO were also observed. It was accepted that high electron density of metallic Pd helped the strengthening of M–C bond through the formation of a metal-CO covalent adduct, which transferred electron into the anti bonding 2u* orbits and weakens the C–O bond[52]. As metallic Pd was partially oxidized, the electron

density of Pd surface decreased and the transferring electron into the anti bonding 2u* orbits of C–O bond was suppressed, which could lead to the blue shift of Pd^0_2-CO. After removal of CO from the feed gas, the vibration peaks of Pd^+_2-CO, Pd^0_2-CO and Pd^0-COdisappear, which indicated the adsorbed CO was consumed by oxygen in the feed gas.

For CO adsorption on NC, as shown in Fig. 5b, a weak and broad Pd^{2+}-CO band could be observed around 2166 cm^{-1}, the CO adsorption amount was much smaller than that on NCR. Although XPS results in Fig. 3 displayed the surface Pd species of NC existed as PdO, a linear Pd^0-CO band could be clearly detected at 2090 cm^{-1}, and the peak intensity increased slightly with the CO adsorption time, which implied that part PdO could be reduced to Pd^0 by CO in the CO adsorption. It was different to the bridge adsorption of CO on NCR (Pd^0_2-CO), CO was mainly linearly adsorbed on the Pd sites of NC. It was because that CO in the feed gas could reduce a little PdO to Pd metal, the initial long distance between two Pd atoms in partial reduced NC did not allow CO to adsorb on bridge sites.The presence of 10% O_2 did not significantly influence the CO adsorption on NC until O_2 content increased to 40%. A broad Pd^+_2-CO was clearly detected along with the decreasing of Pd^0-CO, and Pd^{2+}-CO was slightly strengthened simultaneously, which indicated a little metallic Pd was re-oxidized to Pd^+ or Pd^{2+} by O_2. After removing CO from the feed gas, Pd^+_2-CO and Pd^0-CO still could be observed, which indicated Pd^+_2-CO and Pd^0-CO on NC were inactive in room temperature.

For CO adsorption on CF (Fig.5c), a sharp peak of Pd^+_2-CO and weak peaks of Pd^0_2-CO and Pd^0-CO were observed at 1939, 1990 and 2093 cm^{-1}, respectively. The results of XPS showed the surface Pd species were ascribed to Pd^{2+} and Pd^+, but Pd^{2+}-CO could not be detected here. Following the increase of CO adsorption time, the Pd^+_2-CO band grew up quickly, meanwhile, the weak peaks of Pd^0_2-CO and Pd^0-COincreased slightly, which indicated Pd^{2+} in CF was easily reduced into Pd^+ by CO at room temperature. Compared with the CO adsorption on NC, the reduction degree of Pd species greatly depended on the chemical enviroment of Pd. the surrounding ligand of Cl^- could promote the reduction of Pd^{2+} in CF. The intensities of Pd^+_2-CO, Pd^0_2-CO and Pd^0-CO decreased gradually with the increase of O_2 content to 40%. After removing CO from the feed gas, most of the CO adsorption species faded away.

As for CC sample, XPS revealed the surface Pd species were mainly PdO on CC, the rest of Pd were consisted of a large amount of Pd^+ and a little Pd^{2+} closely connected by the residual Cl^- . As shown in Fig.5d, Pd^{2+}-CO was hardly detected in CO adsorption on CC. A sharp Pd^+_2-CO and weak Pd^0_2-CO and Pd^0-CO were observed at 1939 cm^{-1} , 1990 cm^{-1} and 2093 cm^{-1}, respectively. Different from CO adsorption on CF, the intensity of Pd^+_2-CO didn't increased with the increasing of adsorption time, which indicated some Pd^{2+} had been reduced into Pd^+ by CO at the beginning of CO adsorption. It is worth mentioning that the Pd^+_2-CO intensity ratio of CC/CF was 0.38, close to the XPS result (0.28). After the introduction of O_2, all CO adsorption species, including Pd^+_2-CO, Pd^0_2-CO and Pd^0-CO, decreased gradually.After removing CO from the feed gas, CO adsorption species were hardly detected except a small amount of Pd^+_2-CO.

4. Discussion

The oxidation state of Pd played important role in CO oxidation. In general, the adsorption of CO on metal Pd (Pd^0) is relatively stronger than that of O_2, which leads to the CO surface coverage is higher than O_2 and results in the low activity of Pd^0 for CO oxidation[7, 14]. PdO also showed lower activity for CO oxidation due to absence of CO adsorption[31, 33, 34]. However, the oxidation state of Pd could be varied in the reaction process depended on the reaction conditions and chemical environment of Pd.

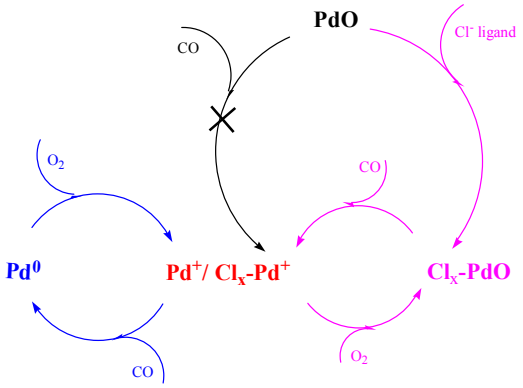

Fig.6 The schematic illustration of catalytic mechanism with different Pd state

For NCR catalyst, XPS results showed the Pd species on the surface was Pd^0, the DRIFTS of CO adsorption on NCR also confirmed it. After introducing of O_2 in the feed flow, part of Pd^0 was easily oxidized to Pd^+ and the adsorption states of CO became more complex (as Fig.6 shown). The significant Pd_2-CO, Pd^+_2-CO and Pd^0-CO were observed instead of only Pd_2-CO in the absence of O_2, which indicated the partial oxidation of Pd^0 produced new adsorption sites for CO. Meanwhile, CO adsorption strength on bridge sites of Pd (Pd^0_2-CO) decreased which corresponding to the blue shift of Pd^0_2-CO. In general, CO preferentially adsorbs on hollow and bridge sites on Pd^0 followed by the top sites, O_2 usually adsorbs on the adjacent adsorption sites on metal Pd[32]. When Pd^0 was partially oxidized by the O_2, the original Pd metal cluster was expanded and the Pd-Pd distance increased, which promoted the transformation of CO adsorption on hollow/bridge sites to the adsorption on the bridge/top sites and resulted in the increase of CO adsorption sites. The combined effects of the increased CO adsorption amount and the decreased CO adsorption strength, deriving from the easily oxidation of Pd^0, led to the higher activity of NCR catalyst for CO oxidation.

It was different from NCR, Pd species existed as PdO on the surface of NC, which proved by the XPS results in Fig.3. PdO hardly adsorbed CO, and PdO was difficult to be reduced by CO to produce new adsorption sites (Fig. 5b), which resulted in the poor activity of NC for CO oxidation[31, 34]. However, for Pd species with high valence, the chemical environment or coordinated ligand of Pd could greatly affect the redox properties and adsorption performance of Pd species (as Fig.6 shown).

For CF catalyst, the XPS results showed the main species of Pd were Pd^{2+} and Pd^+. But unlike PdO, Pd^{2+} coordinated with Cl^- was easily reduced by CO in the reaction gas, corresponding to the enhancement of Pd^+_2-CO vibration and the appearance of

Pd_2-CO with the increasing of CO adsorption time. Furthermore, the Pd^+ species could be stable in the presence of O_2 even if O_2 content increased to 40%.However, Pd^+_2-CO vibration shifted to lower wave number comparing with that on NCR. It indicated the CO adsorption strength on CF was stronger than that on NCR, induced by the effects of Cl^-, which could increase the reaction barrier of CO oxidation[56-58]. Hence, CF showed higher activity for CO oxidation than NC, but lower than NCR.

It is interesting that CC behaved comparable CO oxidation activity with CF and NCR, much higher than NC. XPS results showed the main Pd species was PdO, which should lead to the lower activity for CO oxidation due to the poor adsorption of CO[31, 34]. However, it should be noted that the obvious Cl^- still could be detected on CC catalyst, which promoted the reduction of Pd^{2+} by CO. Compared with CF, catalyst calcination decreased the amount of Cl^- on CC and decreased the reduction properties of Pd species, which along with the relative lower activity for CO oxidation.

In order to further confirm the roles of Cl^- in the CO oxidation on the Pd catalyst, we prepared NCl-C catalysts with the same preparation method of NC catalyst except the adding of hydrochloricacid into $Pd(NO_3)_2$ solution. As can been seen from Fig.7, NCl-C showed much higher activity than NC, which indicated the presence of Cl^- could affect the chemical state of Pd and promote CO oxidation.

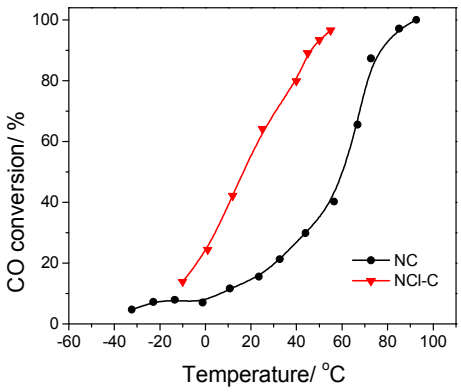

Fig.7 CO oxidation activities of NC and NCl-C (200 ppm CO + 20% O_2 balanced with N_2, WHSV 9,000 ml $(g•h)^{-1}$)

Conclusions

The chemical state of Pd played important role in CO oxidation. We prepared supported Pd catalyst in four different states: metal Pd (NCR), PdO (NC), Pd^{2+} coordinated with Cl^- (Pd^{2+}-Cl, CF), and the mixture of PdO and Pd^{2+}-Cl (CC), and the activity of CO oxidation was in the order of NCR ~ CF > CC >>NC. For metal Pd (Pd^0), partial Pd^0 could be oxidized to Pd ion (Pd^+) by the O_2 in the feed flow, which producing new adsorption sits and increasing CO adsorption amount. Meanwhile, the partial oxidation of Pd decreased CO adsorption strength on Pd surface. The cooperation of enhancement of CO adsorption amount and decrease of CO adsorption strength led to high activity for CO oxidation on NCR. For the Pd with high chemical valence (Pd^{2+}), the chemical environment or coordinated ligand of Pd species showed great effects on the CO oxidation. When Pd^{2+} species existed in the form of PdO, CO was hardly adsorbed on the catalyst surface. Meanwhile, the stable PdO was difficult to be reduced by CO, which indicated the new CO adsorption sites weren't produced in the reaction. The combined effects of these factors led to the poor activity of NC for CO oxidation. However, when Pd^{2+} coordinated with chlorine, Pd^{2+} was much easier to be reduced into Pd^+ by CO than PdO, which greatly promoted CO adsorption and resulted in the good activity for CO oxidation. Furthermore, tuning the CO adsorption by controlling the chemical state of Pd may be a useful approach to prepare the supported Pd catalyst with low temperature CO oxidation activity.

Acknowledgements

This project was supported financially by the National Basic Research Program of China (2010CB732300, 2013CB933201), the National High Technology Research and Development Program of China (2012AA062703), NSFC of China (21171055, 21273150), the New Century Excellent Talents in University (NECT-10-0377), "ShuGuang" Project of Shanghai Municipal Education Commission and Fundamental Research Funds for the Central Universities.

Notes and references

Key Laboratory for Advanced Materials and Research Institute of Industrial Catalysis, East China University of Science and Technology, Shanghai 200237, P. R. China. Fax: +86-21-64253703 E-mail: yunguo@ecust.edu.cn (Y. Guo), wangli@ecust.edu.cn (L. Wang).

1. A. A. Mirzaei, H. R. Shaterian, R. W. Joyner, M. Stockenhuber, S. H. Taylor and G. J. Hutchings, *Catal. Commun.*, 2003, **4**, 17.
2. T. Cheng, Z. Y. Fang, Q. X. Hu, K. D. Han, X. Z. Yang and Y. J. Zhang, *Catal. Commun.*, 2007, **8**, 1167.
3. M. S. Chen and D. W. Goodman,*Science, 2004, 306, 252.*
4. C. J. Jia, Y. Liu, H. Bongard and F. Schüth, *J. Am. Chem. Soc.*, 2010, **132**, 1520.
5. Y. Q. Huang, A. Q. Wang, X. D. Wang and T. Zhang, *Int. J. Hydrogen. Energ.*, 2007, **32**, 3880.
6. B. T. Qiao, L. Q. Liu, J. Zhang and Y. Q. Deng, *J. Catal.*, 2009, **261**, 241.
7. J. Bergeld, B. Kasemo and D. V. Chakarov, *Surf. Sci.*, 2001, **495**, 815.
8. A. Bourane and D. Bianchi, *J. Catal.*, 2001, **202**, 34.
9. B. Qiao and Y. Deng, *Appl. Catal. B-environ.*, 2006, **66**, 241.
10. M. Haruta, N. Yamada, T. Kobayashi and S. Iijima, *J. Catal.*, 1989, **115**, 301.
11. H. Liu, A. I. Kozlov, A. P. Kozlova, T. Shido, K. Asakura and Y. Iwasawa, *J. Catal.*, 1999, **185**, 252.
12. M. Daté, M. Okumura, S. Tsubota and M. Haruta, *Angew. Chem. Int. Edit.*, 2004, **43**, 2129.
13. D. Widmann, R. Leppelt and R. J. Behm, *J. Catal.*, 2007, **251**, 437.
14. I. X. Green, W. Tang, M. Neurock and J. T. Yates, *Science*, 2011, **333**, 736.
15. J. R. Creighton and J. M. White, *Surf. Sci.*, 1982, **122**, 648.
16. W.S. Lee, B.Z. Wan, C. N. Kuo, W. C. Lee and S. Cheng, *Catal. Commun.*, 2007, **8**, 1604.
17. J. S. Lee, E. D. Park and B. J. Song, *Catal. Today*, 1999, **54**, 57.
18. H. Falsig, B. Hvolbæk, I. S. Kristensen, T. Jiang, T. Bligaard, C. H. Christensen and J. K. Nørskov, *Angew. Chem. Int. Edit.*, 2008, **47**, 4835.
19. M. S. Chen, Y. Cai, Z. Yan, K. K. Gath, S. Axnanda and D. W. Goodman, *Surf. Sci.*, 2007, **601**, 5326.
20. A. Bourane and D. Bianchi, *J. Catal.*, 2004, **222**, 499.
21. Q. Fu, W.X. Li, Y. X. Yao, H. Y. Liu, H.Y. Su, D. Ma, X.K. Gu, L. M. Chen, Z. Wang, H. Zhang, B. Wang and X. H. Bao, *Science*, 2010, **328**, 1141.

22. L. Q. Liu, F. Zhou, L. G. Wang, X. J. Qi, F. Shi and Y. Q. Deng, *J. Catal.*, 2010, **274**, 1.
23. B. T. Qiao, A. Q. Wang, M. Takahashi, Y. J. Zhang, J. H. Wang, Y. Q. Deng and T. Zhang, *J. Catal.*, 2011, **279**, 361.
24. L. Liu, B. Qiao, Y. He, F. Zhou, B. Yang and Y. Deng, *J. Catal.*, 2012, **294**, 29.
25. B. Qiao, L. Liu, J. Zhang and Y. Deng, *J. Catal.*, 2009, **261**, 241.
26. W. E. Kaden, W. A. Kunkel, M. D. Kane, F. S. Roberts and S. L. Anderson, *J. Am. Chem. Soc.*, 2010, **132**, 13097.
27. S. K. Kulshreshtha and M. M. Gadgil, *Appl. Catal. B-environ.*, 1997, **11**, 291.
28. T. Iwasawa, M. Tokunaga, Y. Obora and Y. Tsuji, *J. Am. Chem. Soc.*, 2004, **126**, 6554.
29. M. Fernández-García, A. Martínez-Arias, L. N. Salamanca, J. M. Coronado, J. A. Anderson, J. C. Conesa and J. Soria, *J. Catal.*, 1999, **187**, 474.
30. F. X. Liang, H. Q. Zhu, Z. F. Qin, H. Wang, G. F. Wang and J. G. Wang, *Catal. Lett.*, 2008, **126**, 353.
31. K. Zorn, S. Giorgio, E. Halwax, C. R. Henry, H. Gronbeck and G. Rupprechter, *J. Phys. Chem. C*, 2011, **115**, 1103.
32. C. J. Zhang and P. Hu, *J. Am. Chem. Soc.*, 2001, **123**, 1166.
33. M. Cargnello, V. V. T. Doan-Nguyen, T. R. Gordon, R. E. Diaz, E. A. Stach, R. J. Gorte, P. Fornasiero and C. B. Murray, *Science*, 2013, **341**, 771.
34. T. Schalow, B. Brandt, M. Laurin, S. Schauermann, J. Libuda and H.-J. Freund, *J. Catal.*, 2006, **242**, 58.
35. F. Gao, M. Lundwall and D. W. Goodman, *J. Phys. Chem. C*, 2008, **112**, 6057.
36. F. Gao, Y. Wang, Y. Cai and D. W. Goodman, *J. Phys. Chem. C*, 2008, **113**, 174.
37. Y. Guo, G. Z. Lu, Z. G. Zhang, S. H. Zhang, Y. Qi and Y. Liu, *Catal. Today*, 2007, **126**, 296.
38. Y. X. Shen, Y. Guo, L. Wang, Y. Q. Wang, Y. L. Guo, X. Q. Gong and G. Z. Lu, *Catal. Sci. Technol.*, 2011, **1**, 1202.
39. Y. X. Shen, G. Z. Lu, Y. Guo and Y. Q. Wang, *Chem. Commun.*, 2010, **46**, 8433.
40. Y. X. Shen, G. Z. Lu, Y. Guo, Y. Q. Wang, Y. L. Guo and X. Q. Gong, *Catal. Today*, 2011, **175**, 558.
41. H. Q. Zhu, Z. F. Qin, W. J. Shan, W. J. Shen and J. G. Wang, *J. Catal.*, 2005, **233**, 41.
42. A. M. Venezia, L. F. Liotta, G. Pantaleo, V. L. Parol, G. Deganello, A. Beck, Z. Koppány, K. Frey, D. Horváth and L. Guczi, *Appl. Catal. A-gen.*, 2003, **251**, 359.
43. P. Bera, K. R. Priolkar, A. Gayen, P. R. Sarode, M. S. Hegde, S. Emura, R. Kumashiro, V. Jayaram and G. N. Subbanna, *Chem. Mater.*, 2003, **15**, 2049.
44. G. A. Parks, *Chem. Rev.*, 1965, **65**, 177.
45. D. Kim, S. Woo, J. Lee and O. B. Yang, *Catal. Lett.*, 2000, **70**, 35.
46. T. Baidya, G. Dutta, M. S. Hegde and U. V. Waghmare, *Dalton. T.*, 2009, 455.
47. F. Wang and G. X. Lu, *J. Phys. Chem. C*, 2009, **113**, 4161.
48. S. Komhom, O. Mekasuwandumrong, P. Praserthdam and J. Panpranot, *Catal. Commun.*, 2008, **10**, 86.
49. A. S. Ivanova, E. M. Slavinskaya, R. V. Gulyaev, V. I. Zaikovskii, O. A. Stonkus, I. G. Danilova, L. M. Plyasova, I. A. Polukhina and A. I. Boronin, *Appl. Catal. B-environ.*, 2010, **97**, 57.
50. W. J. Shen, M. Okumura, Y. Matsumura and M. Haruta, *Appl. Catal. A-gen.*, 2001, **213**, 225.
51. M. L. Cubeiro and J. L. G. Fierro, *Appl. Catal. A-gen.*, 1998, **168**, 307.
52. H. Q. Zhu, Z. F. Qin, W. J. Shan, W. J. Shen and J. G. Wang, *Catal. Today*, 2007, **126**, 382.
53. M. Fernández-García, A. Martínez-Arias, A. Iglesias-Juez, A. B. Hungría, J. A. Anderson, J. C. Conesa and J. Soria, *Appl. Catal. B-environ.*, 2001, **31**, 39.
54. K. I. Choi and M. A. Vannice, *J. Catal.*, 1991, **127**, 465.
55. F. X. Liang, H. Q. Zhu, Z. F. Qin, G. F. Wang and J. G. Wang, *Catal. Commun.*, 2009, **10**, 737.
56. Y. Guo, Y. Lou, X. M. Cao, J. G. Lan, L. Wang, Q. G. Dai, J. Ma, Z. Y. Zhao, P. J. Hu and G. Z. Lu, *Chem. Commun.*
57. Y. Lou, L. Wang, Y. H. Zhang, Z. Y. Zhao, Z. G. Zhang, G. Z. Lu and Y. Guo, *Catal. Today*, 2011, **175**, 610.
58. Y. Lou, L. Wang, Z. Y. Zhao, Y. H. Zhang, Z. G. Zhang, G. Z. Lu, Y. Guo and Y. L. Guo, *Appl. Catal. B-environ.*, 2014, **146**, 43.

The effect of Pd chemical state on the activity of Pd/Al_2O_3 catalysts in CO oxidation

Yanhui Zhang, Yafeng Cai, Yun Guo*, Haifeng Wang, Li Wang*, Yang Lou, Yanglong Guo, Guanzhong Lu, Yanqing Wang